Sedimentation of charged colloids: The primitive model and the effective one-component approach

Aldemar Torres,[1] Alejandro Cuetos,[2] Marjolein Dijkstra,[2] and René van Roij[1]
[1]*Institute for Theoretical Physics, Utrecht University, Leuvenlaan 4, 3584 CE Utrecht, The Netherlands*
[2]*Soft Condensed Matter, Utrecht University, Princetonplein 5, 3584 CC Utrecht, The Netherlands*
(Received 19 February 2007; published 19 April 2007)

Sedimentation-diffusion equilibrium density profiles of suspensions of charge-stabilized colloids are calculated theoretically and by Monte Carlo (MC) simulations, both for a one-component model of colloidal particles interacting through pairwise screened-Coulomb repulsions and for a three-component model of colloids, cations, and anions with unscreened-Coulomb interactions. We focus on a state point for which experimental measurements are available [C. P. Royall *et al.*, J. Phys.: Condens Matter **17**, 2315 (2005)]. Despite the apparently different picture that emerges from the one- and three-component models (repelling colloids pushing each other to high altitude in the former, versus a self-generated electric field that pushes the colloids up in the latter), we find similar colloidal density profiles for both models from theory as well as simulation, thereby suggesting that these pictures represent different viewpoints of the same phenomenon. The sedimentation profiles obtained from an effective one-component model by MC simulations and theory, together with MC simulations of the multicomponent primitive model are consistent among themselves, but differ quantitatively from the results of a theoretical multicomponent description at the Poisson-Boltzmann level. We find that for small and moderate colloid charge the Poisson-Boltzmann theory gives profiles in excellent agreement with the effective one-component theory if a smaller effective charge is used. We attribute this discrepancy to the poor treatment of correlations in the Poisson-Boltzmann theory.

DOI: 10.1103/PhysRevE.75.041405 PACS number(s): 82.70.Dd, 64.60.Cn, 64.10.+h, 82.39.Wj

I. INTRODUCTION

Colloidal particles with a density different from that of the dispersive medium sediment because of the gravitational force. At fixed temperature T, the resulting nonhomogeneous equilibrium distribution is a consequence of the balance between energy and entropy of the different chemical species involved. This equilibrium is characterized by measurable density profiles [1,2]. In the case of sufficiently dilute suspensions those profiles obey the barometric law $\rho(x) \propto \exp(-x/L)$, with $L=k_BT/mg$ the gravitational length, m the buoyant mass, g the gravitational acceleration, k_B the Boltzmann constant, T the absolute temperature, and $\rho(x)$ the number density of colloids at altitude x. In dense systems, with nonnegligible colloidal interactions, strong deviations from the barometric law have been observed, e.g., for colloidal hard spheres at packing fractions up to and beyond the freezing point [1,3]. More surprisingly (at least initially) were the strong deviations from the barometric law in rather dilute suspensions of highly charged colloids at low salinity [4]. The measured density profiles suggested an extreme enhancement, by at least one order of magnitude, of the apparent mass of the colloids [2,4]. This system was theoretically analyzed in terms of a three-component model of colloids and monovalent cations and anions, for which (modified) Poisson-Boltzmann (PB) theories in gravity revealed a self-consistent electric field that pushes up the colloids to high altitude against gravity [5–10], thereby reducing the apparent mass as observed experimentally. Moreover, the existence of this electric field was confirmed in primitive model simulations [11]. However, another explanation was given more recently in Ref. [12], where hydrostatic equilibrium in a one-component system of colloids interacting through pairwise screened-Coulomb repulsion was considered. In the present paper we investigate the relations between these two pictures in more detail by considering both models (colloid-cation-anion mixture and colloids-only system) by theory as well as Monte Carlo (MC) simulation. For the one-component approach we use a model based on effective pairwise screened-Coulomb interactions. The profiles are obtained from the solution of the hydrostatic equilibrium equation that uses the isothermal compressibility obtained from the solution of the Ornstein-Zernike (OZ) equation with the rescaled mean spherical approximation (RMSA) closure [13]. This approach is similar to that introduced in [12]. In this case, entropic and electrostatic effects are implicitly included in the structure of the suspension (see Sec. II). Furthermore, we perform MC simulations for this model. Within the multicomponent picture, we approach the problem using the Poisson-Boltzmann theory introduced in Ref. [9], which explains the nonbarometric profiles in terms of a macroscopic electric field that appears as a consequence of a charge inhomogeneity [5–11]. We also performed simulations of this system using the primitive model in gravity. These particular simulations require a substantial amount of CPU time since a considerable number of microions has to be taken into account to mimic the substantial salt concentration in the suspension. We focus on a state point for which experimental information is available, and compare the profiles obtained from the mentioned theoretical and numerical approaches with published measurements [2].

The paper is organized as follows. In Sec. II we introduce the one-component model, the structure factor of the suspension determined through RMSA, and we discuss some details regarding the simulation technique of the one-component model. In Sec. III we briefly revise the PB theory for sedimentation, introduce the primitive model in gravity, and some aspects regarding the simulations. Results and discus-

sion are presented in Secs. IV and V, respectively, where we compare the different theoretical and numerical results with experimental data. A summary and conclusions are gathered in Sec. VI.

II. EFFECTIVE ONE-COMPONENT MODEL

Let us consider a system consisting of charged spheres of diameter $\sigma=2a$, mass M, and electric charge $-Ze$, in osmotic contact with a reservoir of 1:1 electrolyte with salt concentration $2\rho_s$. The solvent has mass density ρ_l and is characterized by an electric permittivity ϵ. Let us assume also that the dielectric constant of the spheres and the electrolyte are identical to avoid electrostatic image effects and Van der Waals forces between the spheres. Assuming pairwise effective colloidal interactions, the potential energy part of the Hamiltonian of the effective one-component system of colloids in the presence of gravity is given by

$$H = \sum_{i=1}^{N} mgx_i + \sum_{i<j}^{N} v(r_{ij}), \tag{1}$$

where the first term in the right-hand side is the potential energy of colloid i at height x_i measured from the bottom of the sample. Here $m=M-\rho_l\pi\sigma^3/6$ the buoyant mass of the colloidal particles, and $v(r)$ is the familiar screened-Coulomb potential

$$\beta v(r) = \begin{cases} \infty & \text{if } r < \sigma \\ \dfrac{Z^2 \exp(\kappa\sigma)}{(1+\kappa a)^2} \dfrac{\lambda_B}{r} \exp(-\kappa r) & \text{if } r \geq \sigma, \end{cases} \tag{2}$$

with $\beta=(k_BT)^{-1}$, where k_B is the Boltzmann constant and where $\lambda_B=\frac{\beta e^2}{\epsilon}$ is the Bjerrum length, $\kappa=\sqrt{8\pi\lambda_B\rho_s}$ is the inverse screening length, and r is the distance between centers of colloidal particles. Under isothermal conditions and for small density gradients, the osmotic pressure of the suspension depends only on the local number density of colloids $\rho(x)$. The latter is determined from the nonlinear differential equation that follows from inserting $\rho(x)$ into the hydrostatic equilibrium equation $d\Pi(x)/dx=-mg\rho(x)$ with Π the osmotic pressure of the suspension with respect to the salt reservoir. This yields

$$\frac{d\rho(x)}{dx} + \frac{\chi_T(\rho(x))}{L}\rho(x) = 0, \tag{3}$$

where $\chi_T^{-1}=\left(\frac{\partial(\beta\Pi)}{\partial\rho}\right)_T$ is the inverse of the isothermal compressibility of the bulk fluid and L is the gravitational length defined above. The sedimentation profiles can be obtained by solving Eq. (3) if the function $\chi_T(\rho)$ is known for the relevant density regime. In order to determine $\chi_T(\rho)$ we use the well-known Kirkwood-Buff relation $\chi_T=\lim_{q\to 0} S(q)$ with $S(q)$ the structure factor as calculated by Hansen, Hayter, and Penfold within the RMSA closure of the Ornstein-Zernike equation [13,14]. By this procedure the sedimentation profiles are determined solely from the structure of the effective one-component bulk fluid. Notice that such a scheme was applied successfully to explain the measured hard-sphere density profiles in Ref. [1]. For later comparison we also consider an alternative expression for $\chi_T(\rho)$, which is based on the Donnan equation of state as, e.g., given in Ref. [9]. This yields

$$\chi_T^{-1} = 1 + \frac{Z^2\rho/2\rho_s}{\sqrt{1+(Z\rho/2\rho_s)^2}}, \tag{4}$$

which features the high-density or low-salt limit $\chi_T(\rho)=1+Z$ for $Z\rho \gg 2\rho_s$, such that insertion into Eq. (3) yields $\rho(x) \propto \exp[-x/(Z+1)L]$, i.e., an effective gravitational length that is a factor $Z+1$ larger than that in the barometric law [9]. The remaining task in order to find the sedimentation profiles is to insert χ_T into Eq. (3) and to solve the nonlinear equation numerically on an x grid.

In addition we perform standard Monte Carlo simulations of a system described by the interaction Hamiltonian (1) for the parameters $Z=76$, colloid diameter $\sigma=1.91$ μm, Bjerrum length $\lambda_B=10.4$ nm, screening parameter $\kappa\sigma=1.2$, and average colloidal packing fraction $\overline{\eta}=H^{-1}\int_0^H \eta(x)dx=0.0053$ with the height $H=50.92\sigma$. The experimental screening parameter satisfies $\kappa\sigma=1.2$. These parameters are identical to those of the experimental system studied in Ref. [2], where $Z=76$ stems from the best fit of the experimental density profile with a theoretical prediction based on the primitive model (see below). The dimensions of the rectangular simulation box are $10\sigma\times 10\sigma\times H$. We checked that the horizontal area was large enough to exclude finite-size effects. We employed periodic boundary conditions in the horizontal directions; in the vertical directions the system is bounded by hard walls that exclude the centers of colloids at $x<0$ and $x>H$.

III. PRIMITIVE MODEL IN GRAVITY

As mentioned in the Introduction, a different approach to study sedimentation profiles is to consider each chemical species separately, namely, colloids (c), coions ($-$), and counterions ($+$). The Hamiltonian of the system can be written as

$$H = H_{cc} + H_{ii} + H_{ci} + \sum_{i=1}^{N} mgx_i, \tag{5}$$

where the first three terms in the right-hand side include colloid-colloid, ion-ion, and colloid-ion pairwise interactions, respectively, and the last term is the gravitational energy of the colloids introduced in Eq. (1); the ions are assumed to be massless. In this model, the electrostatic pair interactions are of the form

$$\beta v_{ij}(r) = \begin{cases} \infty & \text{if } r < \sigma_{ij} = (\sigma_i+\sigma_j)/2 \\ Z_iZ_j\dfrac{\lambda_B}{r} & \text{if } r \geq \sigma_{ij}, \end{cases} \tag{6}$$

with σ_k and Z_k the diameter and the charge number of species $k=\{c,+,-\}$, i.e., $Z_c=-Z$, $Z_+=1$, $Z_-=-1$, $\sigma_c=\sigma$, and $\sigma_+=\sigma_-\ll\sigma$. The number of particles are denoted by N_k, i.e., $N_c=N$ and $N_+=N_-+ZN$ for charge neutrality reasons. This three-component model can be studied within Poisson-

Boltzmann theory [5–10]. The main idea is to relate the density profiles $\rho(x), \rho_+(x), \rho_-(x)$ of the colloids cations and anions, respectively, to the local electrostatic Donnan potential $\psi(x)$ through

$$\rho_\pm(x) = \rho_s \exp[\pm \phi(x)], \tag{7}$$

$$\rho(x) = \rho_0 \exp[-x/L + Z\phi(x)], \tag{8}$$

$$\phi''(x) = \kappa^2 \sinh \phi(x) + 4\pi\lambda_B Z\rho(x), \tag{9}$$

with $\phi(x)$ defined by the dimensionless combination $\phi(x) = e\psi(x)/k_BT$ and where ρ_0 is a normalization constant. Here a prime denotes a derivative with respect to x. Under appropriate conditions, typically $Z^2\rho(x) \gg 2\rho_s$, it was found that $\phi(x)$ is a linear function of x in macroscopically large parts of the system, i.e., there is a constant electric field that lifts the colloids to higher altitudes than expected on the basis of their mass [9]. This result stems both from numerical solutions of Eqs. (7)–(9) and from the "Laplace-Boltzmann" equation, where Eq. (9) is replaced by the local charge neutrality condition $\kappa^2 \sinh \phi(x) + 4\pi\lambda_B Z\rho(x) = 0$. Note that by combining the latter equation with Eqs. (7) and (8) one recovers the hydrostatic equilibrium condition (3) with χ_T given by Eq. (4). On the other hand, the set of equations (7)–(9) can be solved numerically in order to determine the local electrostatic potential $\phi(x)$ together with the equilibrium profile $\rho(x)$ by an iterative procedure as pointed out in [9]. Such a procedure requires two boundary conditions, e.g., $\phi'(0) = \phi'(H) = 0$, where H is the height of the solvent meniscus.

A system described by the Hamiltonian (5) was simulated in a rectangular box of horizontal area $9\sigma \times 9\sigma$ and height $H = 50\sigma$. The vertical coordinate x is restricted to $x \in [0, H]$, and periodic boundary conditions are only applied in the horizontal plane and not in the vertical direction. In order to be as close as possible to the experiments of Ref. [2], we considered colloids with charge $Z = 76$, diameter $\sigma = 1.910$ μm, gravitational length $L = 2.41\sigma$, Bjerrum length $\lambda_B = 10.4$ nm, and average colloidal packing fraction $\overline{\eta} = H^{-1}\int_0^H \eta(x)dx = 0.0053$ (with $H = 50\sigma$). The experimental screening parameter satisfies $\kappa\sigma = 1.2$. This state point is realized, with the present box size and shape, by the number of colloids $N_c = 12$ and the number of positive and negative ions $N_+ = 13\,516$ and $N_- = 12\,604$, respectively. In order to take the long-range electrostatic interactions into account we have employed a combination of Ewald summation in a slab geometry with the lattice method proposed by Panagiotopoulos and Kumar [15]. The parameters of the Ewald summation and lattice method are the same as those in Ref. [16]. Note that the large number of ions, which have to be included to represent the low but yet substantial screening parameter, makes the simulations extremely time consuming.

In a dense system of microions, a simple Monte Carlo move of a colloid would almost certainly result in a hard-core overlap with one of the microions. In order to avoid such overlaps we use a cluster move technique, where ions that overlap with the new colloid position are moved into the space left empty by the displaced colloid, more details on this technique can be found in Refs. [17,18]. The percentage of accepted moves of each component (colloids and microions) was maintained at about 40%. A typical simulation consists of 10^5 MC cycles. Due to the high number of microions, if ions and colloids are chosen with the same probability, the colloids would be almost motionless. To avoid this in order to obtain *colloidal* density profiles with good statistics, each cycle consists of $0.9\mathcal{N}$ trials to move a randomly chosen colloid (together with the microions that are included in the cluster move) and $0.1\mathcal{N}$ trials to move a randomly chosen colloid or microion, with $\mathcal{N} = N + N_+ + N_-$ the total number of microions and colloids in the system. This choice satisfies detailed balance and was tested successfully for the conditions reported in Ref. [16]. To check if the system was equilibrated, the average altitude of the centers of mass of the colloids was monitored in the simulation; when the center of mass was not stable, further equilibration was performed before taking measurements. A final simulation with 2×10^5 MC cycles was performed to obtain averages.

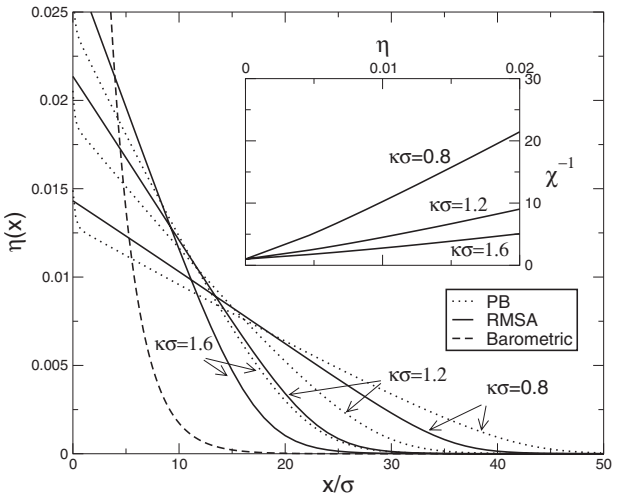

FIG. 1. Colloidal sedimentation profiles based on hydrostatic equilibrium (3) calculated using the RMSA-based compressibility of the one-component Yukawa model, compared to those based on the multicomponent PB theory (7)–(9), for the screening parameters $\kappa\sigma = 0.8$, 1.2, and 1.6. The colloidal charge is $Z = 76$, the colloid diameter is $\sigma = 1.91$ μm, the Bjerrum length is $\lambda_B = 10.4$ nm, the gravitational length is $L = 2.41\sigma$, the average colloid packing fraction is $\overline{\eta} = 0.0053$, and the sample height is $H = 50\sigma$, as reported in Ref. [2]. The dashed curve is the barometric distribution with the same normalization. The inset shows the RMSA-based compressibility.

IV. RESULTS

Figure 1 shows a first comparison of theoretical predictions based on the one-component and three-component models. We see several theoretical sedimentation profiles as a function of the altitude x, corresponding to colloids of diameter $\sigma = 1.91$ μm, and three different salt concentrations characterized by screening parameters $\kappa\sigma = 0.8$, 1.2, and 1.6. All profiles shown in Fig. 1 are for the same gravitational

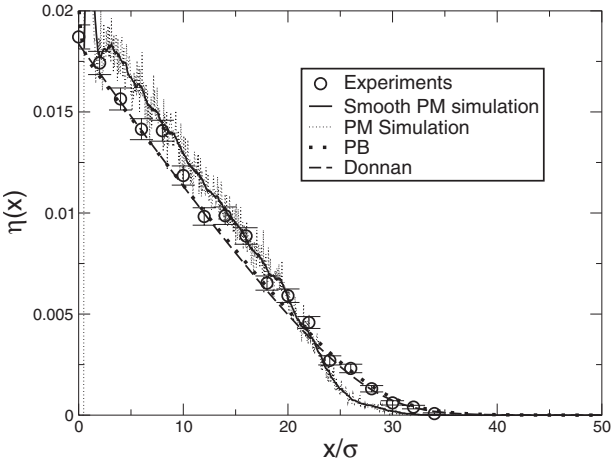

FIG. 2. Colloidal sedimentation density profiles for colloidal charge $Z=76$ stemming from multicomponent PB theory (7)–(9), from the Donnan compressibility (4) combined with hydrostatic equilibrium (3), and simulations of the primitive model in gravity, for the parameters of Fig. 1 and $\kappa\sigma=1.2$. The symbols denote the experimental measurements from Ref. [2].

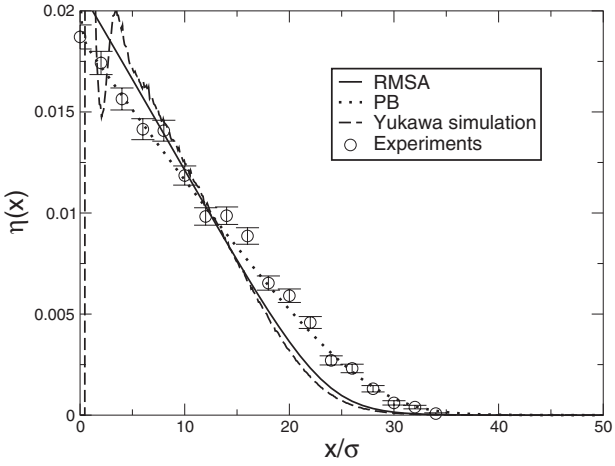

FIG. 3. Sedimentation profiles of the effective one-component Yukawa model calculated using both RMSA and standard MC simulations, compared with the experimental measurements of Ref. [2] and the three-component PB theory, for $Z=76$ and all other parameters as in Fig. 2. Note the close agreement between the two Yukawa results, and their small but systematic deviation from the experiments and the PB theory.

length $L=2.41\sigma$, average packing fraction $\overline{\eta}=0.0053$, sample height $H=50\sigma$, and Bjerrum length $\lambda_B=10.4$ nm. For each $\kappa\sigma$, the colloid density profile is calculated for both the effective one-component model based on the solution of the hydrostatic equilibrium equation (3) using the isothermal compressibility obtained from the RMSA closure, as well as from the multicomponent PB theory described by Eqs. (7)–(9). We also show, for the sake of comparison, the corresponding barometric profile obtained from Eqs. (8) and (9) in the case of uncharged colloids ($Z=0$), for the same normalization. The inset shows the compressibilities as a function of the colloid density, as obtained from the solution of the OZ equation within the RMSA closure. At zero density all the compressibility curves reduce to the ideal-gas compressibility, and with increasing colloid density the electrostatic repulsions manifest themselves as a reduction of χ_T: the weaker the screening, the stronger the effective colloidal interactions. We note that each one-component Yukawa system yields steeper density profiles than those of the corresponding three-component model, for all $\kappa\sigma$ considered here, i.e., the one-component systems have a relatively small average altitude and a relatively low density at higher altitudes. We will argue in more detail below that the source of the difference between the one- and three-component predictions is mainly due to the poor representation of the colloid-colloid correlations in the three-component PB theory.

Figure 2 shows the experimentally measured density profile of Ref. [2] compared to density profiles as obtained from the multicomponent models: the three-component PB theory of Eqs. (7)–(9) and simulation of the primitive model in gravity as introduced in Sec. III. In spite of the fact that the primitive model simulation was equilibrated during about one year CPU time and the measurements were performed over four months CPU time, the level of noise in the raw data is still quite high. Therefore also a smoothed curve of the simulated profile is shown to facilitate comparisons. The difficulty in obtaining good statistics in this particular simulation is due to the fact that the total number of colloids in the system is exceedingly small ($N_c=12$), whereas the total number of particles in the system is rather large (26 132), most of them salt ions, needed to achieve the required screening parameter condition. That the Donnan-based density profile is accurate when compared to the experiments is *only* due to the fact that the experimental value[1] $Z=76$ stems from a fit to PB theory [2], which is equivalent to the Donnan equation of state in the local neutrality "Laplace-Boltzmann" limit as explained below Eqs. (7)–(9). In other words, $Z=76$ is close to a best fit to the Donnan equation of state.

In Fig. 3 we see a first comparison of the sedimentation profile obtained experimentally with sedimentation profiles calculated using the effective one-component models: simulation of the Yukawa system and the RMSA approach of Sec. II. We also include the profiles obtained from the multicomponent PB theory for the sake of comparison. The contrast between the simulations and the experimental curve seems to reveal a systematic deviation such that the simulated and RMSA profiles are actually somewhat too steep. Indeed, when we allow Z to be a fit parameter in the one-component Yukawa system, keeping all the other parameters equal, it turns out that $Z=94$ gives the best the agreement of the one-component models with the experimental profile. It is tempting to conclude, therefore, that $Z=76$ gives merely a best fit to the experiment within PB theory given by Eqs. (7)–(9), which (to a large extent) ignores colloid-colloid correlations, whereas inclusion of these correlations (as in the simulations

[1]The measured density profile was fitted to the predictions of Poisson-Boltzmann theory, and it was concluded in Ref. [2] that the colloidal charge equals $-78e$. Here we concluded that $-76e$ gives the best fit within Poisson-Boltzmann theory, this difference is due to details of the fitting procedure and does not interfere with our arguments.

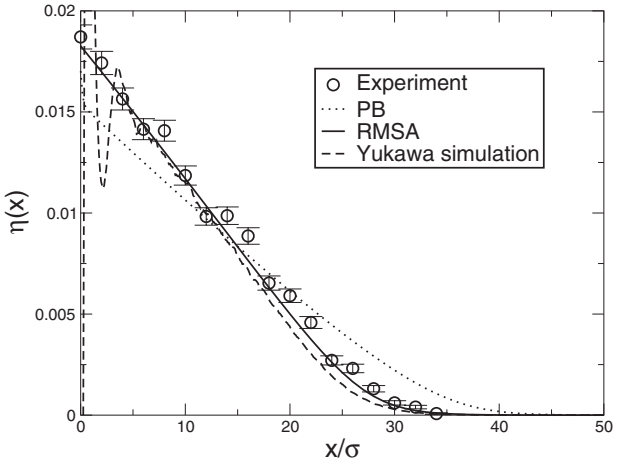

FIG. 4. As in Fig. 3, but with $Z=94$, such that the Yukawa model profiles (both RMSA and simulated) fit the experimental profile best. The PB profile is clearly less accurate now.

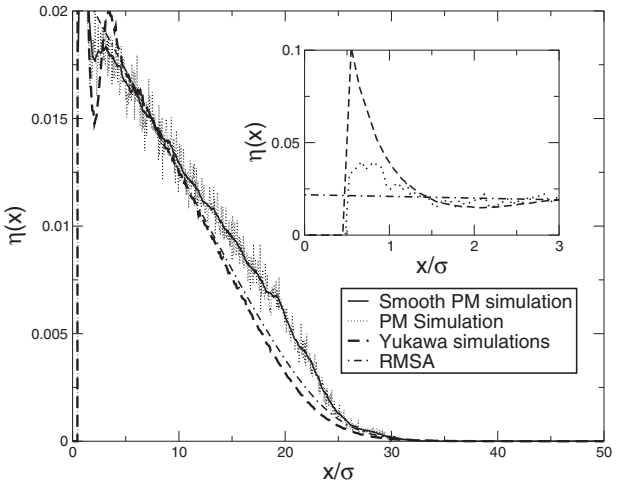

FIG. 5. Sedimentation density profiles as obtained from simulations of the primitive model in gravity and simulations of the Yukawa fluid compared with the one-component RMSA model for colloidal charge $Z=76$ and all other parameters as in Fig. 2. The difference between the profiles can partly be attributed to the structural differences close to the bottom at $x=0$ as shown in the inset, where the simulations reveal a hard-wall induced structure that is not captured by the RMSA-based theory, and perhaps partly by slow equilibration and poor statistics in the simulations due to the small number of colloids.

of the primitive model and that of the Yukawa system, and in the RMSA-based theory) gives rise to a density profile that is systematically steeper in comparison with the experiment.

In Fig. 4 we show the resulting sedimentation profiles based on the Yukawa potential simulations and the RMSA closure for $Z=94$. For comparison we also plot the multicomponent PB model for $Z=94$ revealing a relatively poor agreement with the other curves. In this case the PB approach clearly fails to reproduce quantitatively the sedimentation profiles. On the other hand, the agreement of the experimental profile with the effective one-component models is good, except that as mentioned before, the simulated profile exhibits much more structure close to the hard wall that represents the bottom of the sample in the simulations—this packing effect is not captured by the local-density approximation that underlies the hydrostatic equilibrium condition, and is not seen in the experiment because the actual sample extends beyond the plotted x range.

In Fig. 5 we show sedimentation profiles as obtained by simulations of the primitive model and of the Yukawa model, compared with those by the RMSA approach, all for $Z=76$. The agreement is perhaps a bit less quantitative than one would have expected. One of the reasons that the density in the primitive model is considerably higher in $x/\sigma \in (10,25)$ is due to the structure close to the hard wall at the bottom near $x=0$, as shown in the inset of Fig. 5, where the two Yukawa systems reveal a larger net adsorption than that of the primitive model, albeit for different reasons: the simulated Yukawa system shows a strong peak at $x=\sigma/2$ while the RMSA-based profile continues to be nonzero down to $x=0$. Given that we imposed that $\bar{\eta}$ is identical in all cases, there must also be a region in space where the density in the primitive model exceeds the other two; the order of magnitude of the integrated differences over $x/\sigma \in (10,25)$ is indeed similar to the negative of that over $x/\sigma \in (0,3)$. Another reason for these differences might be the poor statistics and slow equilibration of the primitive model simulations. Recall that the present data are based on about one year of CPU time, so considerable extensions and more checks are not easily obtained. This also prevented us from performing primitive model simulations for $Z=94$.

V. DISCUSSION

The first observation from Fig. 3 should be the gross agreement between the experiments and all calculated and simulated profiles. In all cases we have $\kappa\sigma=1.2$, Bjerrum length $\lambda_B=10.4$ nm, colloid diameter $\sigma=1.91$ μm, and gravitational length $L=2.41\sigma$. The colloidal charge is taken as $Z=76$, and the measured packing fractions are in the range $0<\eta(x)<0.02$, where $\eta(x)=(\pi/6)\sigma^3\rho(x)$. This regime is such that $Z\rho(x)/2\rho_s<0.17$ for all x, i.e., even at the highest density the ion concentration is dominated by the reservoir salt concentration $2\rho_s$, such that the screening constant is indeed essentially a constant independent of the height or density, as implicitly assumed in Eq. (2). A closer look, however, shows that even though the simulations and the RMSA result of the Yukawa system are very close to each other (except at the bottom where packing effects affect the simulations), they both deviate systematically from the experiment: the former two are too steep and have too low a density at higher altitudes. From the fact that the RMSA-based profile and that of the Yukawa simulations are so close to each other, one could conclude that they are mutually consistent and both accurate, and that their deviation from the experiment is mainly due to the present choice of $Z=76$, which was based on the fitting to the PB theory of Eqs. (7)–(9). This fitting is not optimal due to the inadequacy of the present PB theory to account for correlations among the different species in the system. In particular, PB theory overestimates the colloid density at high altitudes for a given value of Z. This happens for charges $Z \gtrsim 50$, whereas for smaller values of the colloid charge the agreement between the profiles obtained from the PB and RMSA approaches is

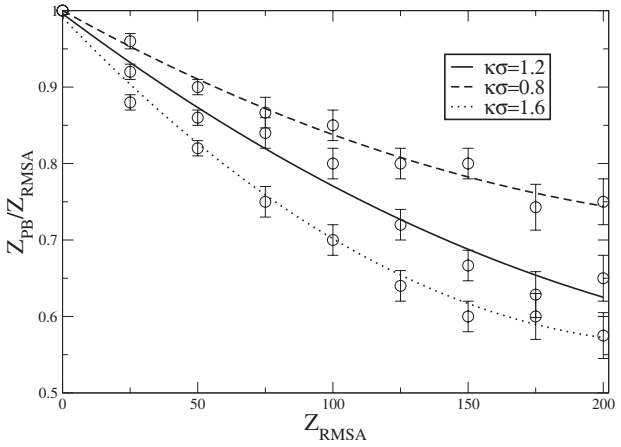

FIG. 6. Ratio of the best-fitting colloidal charge $Z=Z_{PB}$ (see the text) and that of the RMSA charge Z_{RMSA}, as a function $Z_{RMSA} \in (0,200)$, with σ, λ_B, L, $\bar{\eta}$, and H as in Fig. 1, for various screening parameters $\kappa\sigma$. Note that PB theory is increasingly better for lower colloidal charges and lower salt concentrations. The lines are mere guides for the eye.

excellent, as far as an effective (smaller) value for the charge is used in the PB approach as discussed in detail below. For the parameters of present interest, fitting the experimental density profile to that of the Yukawa system treated within the RMSA closure, we concluded that $Z=94$ gives the best fit.

Given that a Yukawa system with a colloidal charge $Z=Z_{RMSA}=94$ is best described within PB theory by a colloidal charge $Z=Z_{PB}=76$, for the present system parameters, it is interesting to investigate the relation between Z_{RMSA} and Z_{PB} for other values of the colloid charge. In Fig. 6 we plot the ratio Z_{PB}/Z_{RMSA} for $0<Z_{RMSA}<200$, for three screening constants while all the other parameters are left unchanged. Figure 7 shows the corresponding density profiles for $\kappa\sigma=1.2$ and $Z_{RMSA}=200$, 94, and 40. One can conclude that for $Z_{RMSA} \lesssim 50$, PB theory reproduces the RMSA-Yukawa sedimentation profiles very accurately provided the colloidal charge Z_{PB} is reduced by up to 20% of Z_{RMSA}. Note that the

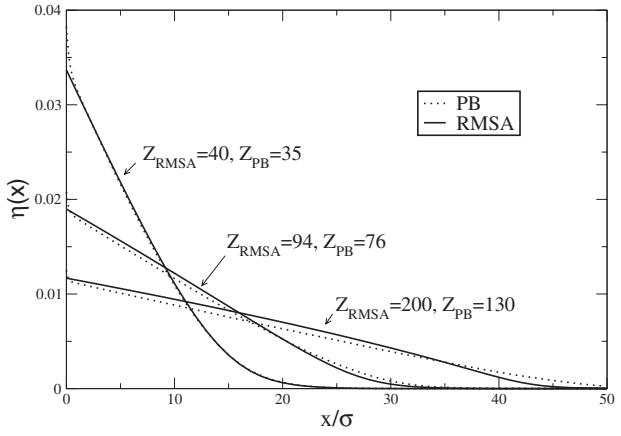

FIG. 7. Sedimentation profiles obtained from RMSA theory compared to those of PB theory using the best-fitting Z_{PB} from Fig. 6, for $\kappa\sigma=1.2$ and all the other parameters as in Fig. 6. Note that the quality of the fit detoriates slightly with increasing Z_{RMSA}.

average density here is low enough that the profile in the limit of $Z_{RMSA} \to 0$ becomes essentially barometric; at higher average packing fractions one also expects $Z_{PB}/Z_{RMSA} \neq 1$ in this limit, due to hard-core effects that are not accounted for properly in the PB theory. The required reduction of Z_{PB}/Z_{RMSA} with increasing $Z_{RMSA}>50$ exceeds 20%, and, in addition, the quality of the best-fitting PB profile (quantified by the mean-squared deviation) becomes slightly less satisfactory as is reflected by the increase of the error bars in Fig. 6 with increasing Z_{RMSA}; this is also shown in Fig. 7.

The difference between Z_{RMSA} and Z_{PB} in the present system is of course considerable and significant, but not qualitative. The seemingly different mechanisms that underly the lifting of the colloids to higher altitudes than given by the barometric distribution, as predicted by the three- and one-component theory, should therefore be actually equivalent: the self-consistent electric field that is generated by a net charge imbalance at the boundaries of the three-component system such that the colloids are pushed upwards is merely another way of describing a pairwise screened-Coulomb repulsion that pushes the colloids apart to higher altitudes in a one-component model. This is in line with conclusions in Ref. [12].

We have attributed the difference between the best fit for Z based on Poisson-Boltzmann theory and the other three methods (simulations of the primitive model, and simulations and RMSA theory of the one-component Yukawa system) to the poor account of correlations in the Poisson-Boltzmann theory. In principle, however, there could be other sources that cause such a difference, e.g., charge renormalization and hard-core exclusion effects for the screening ions. Charge renormalization due to nonlinear screening effects [19] is, however, *not* a candidate here to explain the difference for at least two reasons: (i) The actual bare charge is usually larger than the renormalized charge that appears in the prefactor of the screened-Coulomb interactions, whereas here the former seems to be smaller. (ii) The present parameters here are such that $Z\lambda_B/a<1$, whereas charge renormalization is only substantial if this dimensionless combination exceeds about five or so [19–21]. A mechanism whereby the effective colloidal charge is increased was discussed in Refs. [23,22], and is based on the hard-core exclusion of the screening ions at sufficiently high colloid packing fractions: the screening is therefore less effective, which appears as an increase of the effective colloidal charge. However, applying the analysis of Ref. [23] to the present case gives only marginally larger values of the effective charge, by less than 1% at the highest density $\eta \simeq 0.02$. In other words, it appears that this effect cannot explain the difference between $Z=76$ and $Z=94$, leaving the poor account of colloid-colloid correlations in the Poisson-Boltzmann theory as the most plausible source of the difference.

It is interesting to inquire whether the one- and three-component models would also produce essentially the same sedimentation profiles for other sets of parameters than considered here, and whether the hydrostatic equilibrium condition (3) and the Poisson-Boltzmann theory (7)–(9) for the one-component and the three-component case, respectively, produce reliable profiles in all circumstances. In order to answer these questions we consider the regimes of extremely

low and extremely high salt concentrations. First, the potential energy part of the Hamiltonian (1) for the effective one-component system is pairwise additive, which is expected to be a good approximation for the present parameter set where $\kappa\sigma > 1$ and $Z\rho/2\rho_s < 1$, i.e., the range of the interactions is smaller than the size of the particles and the background electrolyte concentration dominates the counterion concentration. At lower salt concentrations, such that $\kappa\sigma \ll 1$ and/or $Z\rho/2\rho_s > 1$, one would expect effective many-body interactions to become relevant [21,24], such that Eq. (1) is not necessarily a reliable effective Hamiltonian anymore. In such an extremely low-salt regime, which is realized in salt-free systems, the Poisson-Boltzmann theory proved to be quantitatively accurate, at least in comparison with simulations [11,25] at low Coulomb couplings. It is interesting to see if the pairwise one-component description is capable of describing the density profiles in this case. We wish to stress here that the possible breakdown of the pairwise screened-Coulomb picture does *not* imply that the system can no longer be seen as a one-component system in hydrostatic equilibrium as described by Eq. (3) with a compressibility that follows from the Kirkwood-Buff relation $S(0)=\chi_T$: these relations remain valid (the former only within the local-density approximation, but given the long screening length in the extremely low-salt regime this approximation is probably accurate). The breakdown would "merely" imply that it is not obvious how to calculate the compressibility or the structure factor without detailed knowledge of the effective Hamiltonian. Second, let us consider the opposite high-salt regime such that $\kappa\sigma \gg 1$ and $Z\rho \ll 2\rho_s$. In this regime the electrostatic interactions are completely screened over distances much smaller than the colloidal diameter, such that the effective one-component system is essentially a (pairwise) hard-sphere system (for water at room temperature at least, where ion-ion correlations are not all that important). In this regime the one-component description based on Eq. (3) is far superior over the PB theory of Eqs. (7)–(9). This is directly seen by regarding the $Z=0$ limit of Eqs. (7)–(9), which reduce to $\phi(x)=0$ and $\rho(x)=\rho_0 \exp[-x/L]$, i.e., the sedimentation profiles become barometric; the hard-core correlations are left out completely from this theory. By contrast, the RMSA closure is, in this hard-core limit, equivalent to the Percus-Yevick closure, and in combination with Eq. (3) the density profiles of hard-sphere sedimentation equilibrium are well described [1,3]. Moreover, also in the present regime with $\kappa\sigma \simeq 1$ the one-component theory performs better. We are currently working on the formulation of a theory that is able to describe sedimentation density profiles in both the high-salt and the low-salt regime on the same footing.

VI. SUMMARY AND CONCLUSIONS

In this paper we have studied sedimentation equilibrium of charge-stabilized colloids at nonzero salt concentration. We compared experimental results with theoretical and simulated profiles obtained on the basis of two models. On one hand a multicomponent model of pointlike colloids, cations, and anions interact with bare Coulomb potentials. For this model we considered a Poisson-Boltzmann theory of the three-component mixture and performed MC simulations using 12 colloids and a total of about 26 132 particles to guarantee the electroneutrality of the system. On the other hand we considered an effective one-component model of colloids interacting by an effective screened-Coulomb potential. For this model we employed a theory based on hydrostatic equilibrium, where the isothermal compressibility is given by the Kirkwood-Buff relation as obtained from the solution of the Ornstein-Zernike equation with the rescaled mean spherical approximation (RMSA) closure for the screened-Coulomb potential. For the effective one-component Yukawa model, we also performed simulations of sedimentation profiles.

The sedimentation profiles obtained from the one-component RMSA theory, simulations of the Yukawa system, and simulations of the primitive model are essentially consistent among themselves but differ from the results of the Poisson-Boltzmann theory. The PB theory shows good agreement with the experiments only because the numerical value of the charge was estimated as to give the best fitting according to this theory. In fact, we have seen that PB theory actually overestimates the colloid density at high altitudes compared to the corresponding Yukawa system, for identical values of Z, at the parameters of interest here. Agreement between PB theory and Yukawa systems can be obtained by reducing the colloidal charge in the PB theory compared to that of the Yukawa model. For small values of the colloid charge, $Z \lesssim 50$ or so, the agreement between the resulting profiles obtained from the PB and RMSA approach is truly excellent, for larger charges up to say $Z=200$ the agreement is still good though somewhat less quantitative as regards the functional form. The CPU time required for the simulation of the multicomponent primitive model and the effective one-component Yukawa model varies between about one year in the former case and one hour in the latter. This shows that theory and simulations of sedimentation profiles on the basis of the effective one-component potential and the Poisson-Boltzmann theory (possibly with a reduced effective charge when colloid-colloid correlations are important) are considerably more efficient than primitive model simulations. In spite of the fact that we have only considered a particular case study, this is presumably true in general, with the Yukawa model probably more accurate when $\kappa\sigma \gtrsim 1$ while PB theory could be more accurate or efficient when $\kappa\sigma \ll 1$. In a future publication we will report on a theory which allows one to interpolate smoothly between these two regimes.

ACKNOWLEDGMENTS

It is a pleasure to thank Alfons van Blaaderen and Paddy Royall for collaborations and sharing their sedimentation profiles data with us. This work is part of the research program of the Stichting voor Fundamenteel Onderzoek der Materie (FOM), which is financially supported by the Nederlandse Organisatie voor Wetenschappelijk Onderzoek (NWO). NWO-CW is acknowledged for the TOP-CW funding.

[1] R. Piazza, T. Bellini, and V. Degiorgio, Phys. Rev. Lett. **71**, 4267 (1993).
[2] C. P. Royall, R. van Roij, and A. van Blaaderen, J. Phys.: Condens. Matter **17**, 2315 (2005).
[3] M. A. Rutgers, J. H. Dunsmuir, J. Z. Xue, W. B. Russel, and P. M. Chaikin, Phys. Rev. B **53**, 5043 (1996).
[4] A. P. Philipse and G. H. Koenderink, Adv. Colloid Interface Sci. **100-102**, 613 (2006).
[5] T. Biben and J.-P. Hansen, J. Phys.: Condens. Matter **6**, A345 (1994).
[6] G. Téllez and T. Biben, Eur. Phys. J. E **2**, 137 (2000).
[7] G. Téllez, J. Chem. Phys. **106**, 8572 (1997).
[8] H. Löwen, J. Phys.: Condens. Matter **10**, L479 (1998).
[9] R. van Roij, J. Phys.: Condens. Matter **15**, S3569 (2003).
[10] J. Zwanikken and R. van Roij, Europhys. Lett. **71**, 480 (2005).
[11] A.-P. Hynninen, R. van Roij, and M. Dijkstra, Europhys. Lett. **65**, 719 (2004).
[12] L. Belloni, J. Chem. Phys. **123**, 204705 (2005).
[13] J.-P. Hansen and J. B. Hayter, Mol. Phys. **46**, 651 (1982).
[14] J. B. Hayter and J. Penfold, Mol. Phys. **42**, 109 (1981).
[15] A. Z. Panagiotopoulos and S. K. Kumar, Phys. Rev. Lett. **83**, 2981 (1999).
[16] A. Cuetos, A.-P. Hynninen, J. Zwanikken, R. van Roij, and M. Dijkstra, Phys. Rev. E **73**, 061402 (2006).
[17] V. Lobaskin and K. Qamhieh, J. Phys. Chem. B **107**, 8022 (2003).
[18] A.-P. Hynninen and M. Dijkstra, J. Chem. Phys. **123**, 244902 (2005).
[19] S. Alexander, P. M. Chaikin, P. Grant, G. Morales, P. Pincus, and D. Hone, J. Chem. Phys. **80**, 5776 (1984).
[20] E. Trizac, L. Bocquet, M. Aubouy, and H. von Grünberg, Langmuir **19**, 4027 (2003).
[21] B. Zoetekouw and R. van Roij, Phys. Rev. E **73**, 021403 (2006); Phys. Rev. Lett. **97**, 258302 (2006).
[22] H. Löwen and G. Kramposthuber, Europhys. Lett. **23**, 637 (1993).
[23] L. Belloni, J. Chem. Phys. **85**, 519 (1986).
[24] C. Russ, H. H. von Grünberg, M. Dijkstra, and R. van Roij, Phys. Rev. E **66**, 011402 (2002).
[25] M. Dijkstra, J. Zwanikken, and R. van Roij, J. Phys.: Condens. Matter **18**, 825 (2006).